ISBN: 978-3-95450-247-9 ISSN: 2673-5490 doi: 10.18429/JACoW-IPAC2024-TUPR54

TRANSIENT FINITE-ELEMENT SIMULATIONS OF FAST-RAMPING MUON-COLLIDER MAGNETS*

D. Moll†, J. Christmann, L. A. M. D'Angelo, H. De Gersem, TU Darmstadt, Germany
F. Boattini, L. Bottura, CERN, Geneva, Switzerland
M. Breschi, University of Bologna, Italy

Abstract

Conceptual studies for a muon collider identify fast-ramping magnets as a major design challenge. Rise rates of more than 1 T/ms are attainable with normal-conducting magnets, incorporating iron yokes to make sure that stored magnetic energies and inductances stay below reasonable thresholds. Moreover, for energy efficiency, the magnets need to exchange energy with capacitors, such that the electric grid only needs to compensate for the losses. The design of such magnet systems is based on two- and three-dimensional finite element models of the magnets coupled to circuit models of the power-electronics equipment. The occurring phenomena necessitate nonlinear and transient simulation schemes. This contribution presents the analysis of a two-dimensional, nonlinear and time transient analysis of a bending magnet, energized by a symmetrical current pulse of a few ms. The magnet yoke is represented by a homogenized material refraining from the spatial discretization of the individual laminates, but nevertheless representing the true eddy-current and hysteresis losses.

INTRODUCTION

Synchrotron acceleration of stable particles and ions is a well established practice at accelerator facilities. Different types of bending magnets keep the particles on a stable orbit and RF cavities increase their energy. As the particle energy is increasing, also the magnetic flux density applied to the beam has to rise. Ramping magnets have therefore always been an integral component of synchrotrons. However, the utilized rise rates have been kept moderately small in order to reduce eddy-current and hysteresis losses.

The muon collider is the most promising pathway towards lepton experiments at particle energies of 10 TeV [1]. Muons are charged elementary particles with an average lifetime of 2.2 µs at rest. The resulting beam loss due to the decay of muons shall remain below acceptable limits. Therefore, the acceleration time measures only a few ms, which lets the dynamic behavior become the crucial characteristic of fast-ramping magnets.

The required dipole magnets of the second rapid cycling synchrotron (RCS2) are supposed to deliver a symmetric ramp from −1.8 T up to 1.8 T within 1 ms at a repetition rate of 5 Hz [2]. These normal-conducting magnets will be positioned in a cascade with high temperature superconducting (HTS) dipoles, which effectively offset the flux experienced by the particles by its constant field [3].

In the following section, we derive how fast-ramping magnets can be modeled numerically. Lastly, the described routine is employed for one preliminary dipole design.

FAST-RAMPING MAGNETS

Magnet Model

One quarter of a fast-ramping *hourglass* dipole magnet [4] is shown in Fig. 1. The beam path along the center of the air gap is enclosed by a beam pipe to simplify the decompression. The iron core is composed of laminates (bright yoke and dark pole). It is used to guide the magnetic flux and thereby reduce the total stored magnetic energy, and limits the technically affordable flux density to 2 T. Conductors (orange exterior, here two per quarter) are responsible to excite the magnet and interact with the power supply.

Formulation

The vector potential approach resolves the magnetic law of Gauss and the law of Faraday-Lenz by

$$\mathbf{B} = \nabla \times \mathbf{A}$$
$$\mathbf{E} = -\dot{\mathbf{A}} - \nabla \phi$$

with $\dot{\mathbf{A}} = \frac{\mathrm{d}\mathbf{A}}{\mathrm{d}t}$ and $\mathbf{A}$ being the magnetic vector potential, ϕ as the electric scalar potential, $\mathbf{B}$ as the magnetic flux density and $\mathbf{E}$ as the electric field strength. The excitation of the N conductors is expressed by

$$-\nabla \phi = \sum_{n=1}^{N} u_n \mathbf{x}_n$$

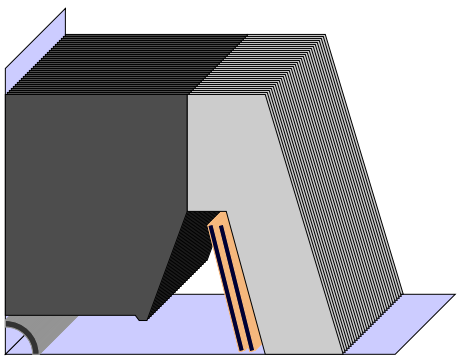

Figure 1: One quarter of an hourglass type dipole magnet.

* endorsed by the IMCC.
† dominik.moll1@tu-darmstadt.de

ISBN: 978-3-95450-247-9 ISSN: 2673-5490 doi: 10.18429/JACoW-IPAC2024-TUPR54

with u_n as the voltage drops and $\mathbf{x}_n$ as voltage distribution functions [5]. We use the constitutive relationships

$$\mathbf{H} = \nu(|\mathbf{B}|^2)\mathbf{B} + \lambda(|\dot{\mathbf{B}}|^2)\dot{\mathbf{B}},$$
$$\mathbf{J} = -\sigma\dot{\mathbf{A}} + \sum_{n=1}^{N} u_n \sigma \mathbf{x}_n. \quad (1)$$

Here, ν is the reluctivity, the term with the coefficient λ models the hysteresis losses and the eddy-current losses caused by magnetic field components along the core laminations, whereas the conductivity σ contains only components in the lamination plane and, thus, models the eddy-current losses due to the perpendicular magnetic field component. Homogenizaion approaches of this kind are well understood, especially for harmonic conditions [6, 7].

Finite Element Model

The magnetic vector potential $\mathbf{A}$ in the computational domain Ω is expressed in terms of N_{FE} many time-dependent coefficients a_k and space-dependent basis functions $\mathbf{w}_k \in H(\mathrm{curl}, \Omega)$,

$$\mathbf{A} = \sum_{k=1}^{N_{\mathrm{FE}}} a_k \mathbf{w}_k.$$

In addition, we define $\mathbf{v}_k = \nabla \times \mathbf{w}_k$ and find $\mathbf{B} = \sum_k a_k \mathbf{v}_k$. The Taylor expansion of $\mathbf{H}$ at guess $\mathbf{A}'$ (with time derivative $\dot{\mathbf{A}}'$) yields

$$\mathbf{H}|_{\mathbf{A}} \approx \mathbf{H}|_{\mathbf{A}'} + \sum_{k=1}^{N_{\mathrm{FE}}} \left(\nu_{\mathrm{d}}|_{\mathbf{A}'}\delta a_k + \lambda_{\mathrm{d}}|_{\mathbf{A}'}\delta\dot{a}_k\right)\mathbf{v}_k$$

with $\delta a_k = a_k - a_k'$, $\delta\dot{a}_k = \dot{a}_k - \dot{a}_k'$,

$$\nu_{\mathrm{d}} = \nu + \frac{\mathrm{d}\nu}{\mathrm{d}|\mathbf{B}|^2} 2\mathbf{B}\mathbf{B}^\top,$$
$$\lambda_{\mathrm{d}} = \lambda + \frac{\mathrm{d}\lambda}{\mathrm{d}|\dot{\mathbf{B}}|^2} 2\dot{\mathbf{B}}\dot{\mathbf{B}}^\top.$$

We can generate N_{FE} equations by expressing Ampère's law in the weak form with test functions $\mathbf{w}_k$

$$\mathbf{h}' + \mathbf{K}_{\nu_{\mathrm{d}}}\delta\mathbf{a} + \mathbf{K}_{\lambda_{\mathrm{d}}}\delta\dot{\mathbf{a}} = \mathbf{X}_\sigma\mathbf{u} - \mathbf{M}_\sigma\dot{\mathbf{a}}.$$

Defining a guess of the voltage $\mathbf{u}'$ allows us to rearrange all unknown increments at the left-hand side

$$\mathbf{K}_{\nu_{\mathrm{d}}}\delta\mathbf{a} + \left(\mathbf{K}_{\lambda_{\mathrm{d}}} + \mathbf{M}_\sigma\right)\delta\dot{\mathbf{a}} - \mathbf{X}_\sigma\delta\mathbf{u} = \mathbf{X}_\sigma\mathbf{u}' - \mathbf{M}_\sigma\dot{\mathbf{a}}' - \mathbf{h}'. \quad (2)$$

The matrix entries are obtained as $\mathbf{K}_\alpha|_{ij} = \int_\Omega \alpha\mathbf{v}_i \cdot \mathbf{v}_j \mathrm{d}\Omega$, $\mathbf{M}_\alpha|_{ij} = \int_\Omega \alpha\mathbf{w}_i \cdot \mathbf{w}_j \mathrm{d}\Omega$, $\mathbf{X}_\sigma|_{ij} = \int_\Omega \sigma\mathbf{w}_i \cdot \mathbf{x}_j \mathrm{d}\Omega$ and $\mathbf{h}'|_i = \int_\Omega \mathbf{H}|_{\mathbf{A}'} \cdot \mathbf{w}_i \mathrm{d}\Omega$. Additional N equations are found by integrating Eq. (1) over the conductor crosssections. In a two-dimensional analysis this yields

$$\delta\mathbf{I} - \mathbf{G}\delta\mathbf{u} + \mathbf{X}_\sigma^\top\delta\dot{\mathbf{a}} = -\mathbf{I}' + \mathbf{G}\mathbf{u}' - \mathbf{X}_\sigma^\top\dot{\mathbf{a}}' \quad (3)$$

with $\mathbf{G}$ as diagonal matrix storing the conductances $G_n = \int_\Omega \sigma\mathbf{x}_n \cdot \mathbf{x}_n \mathrm{d}\Omega$. The problem is well defined if a set of N circuit equations is provided. In this investigation, we connect the conductors to ideal current sources of a time-dependent current I_{s}. We find

$$\delta\mathbf{I} = -\mathbf{I}' + \mathbf{I}_{\mathrm{s}}. \quad (4)$$

Time Integration

A first order time integration scheme allows us to approximate $\dot{\mathbf{a}} = \frac{\mathbf{a}-\mathbf{a}_0}{\Delta t}$ with $\mathbf{a}_0$ as the components of the vector potential $\mathbf{A}$ at the previous time instance. We conclude $\delta\dot{\mathbf{a}} = \frac{\delta\mathbf{a}}{\Delta t}$. It is hence possible to retrieve the unknown increments $\delta\mathbf{I}$, $\delta\mathbf{u}$ and $\delta\mathbf{a}$ by solving the nonlinear system of equations (2-4) for every instance in time with a Newton-Raphson scheme.

APPLICATION

Geometry

A two-dimensional slice of an hourglass magnet with a 30 mm × 100 mm sized air gap was investigated. In every quarter, two adjacent conductor bars of dimensions 140 mm × 3.5 mm are placed 10 mm afar from the yoke (also shown in Fig. 5). A beam pipe was not considered.

Material

The conductors are composed of copper. A fixed temperature working point of 300 K was assumed. The yoke and pole are considered to be manufactured of M235-35A10 laminates, for which the material model is specified by [8]

$$\nu = p_0 + \frac{1\,\mathrm{Am}}{1\,\mathrm{Vs}}(p_1|\mathbf{B}|^2)^{p_2} \quad \text{and} \quad \lambda = p_3 + \frac{p_4}{\sqrt{p_5^2 + |\dot{\mathbf{B}}|^2}}.$$

In this contribution, we apply homogeneous parameters $p_0 = 66.31\frac{\mathrm{Am}}{\mathrm{Vs}}$, $p_1 = 2.6\,\mathrm{T}^{-2}$, $p_2 = 4.2$ that mimic the anhysteretic *BH* curve of the selected material. The parameter $p_5 = 1\,\mathrm{mT/s}$ was chosen small such that $p_3 = 17.1{\times}10^{-3}\frac{\mathrm{Am}}{\mathrm{V}}$ and $p_4 = 125.4\frac{\mathrm{Am}}{\mathrm{V}}$ could be obtained by comparing the averaged loss density with that of the Bertotti loss formula [9]

$$(P_{\mathrm{eddy}})_{\mathrm{avg}} = (p_3|\dot{\mathbf{B}}|^2)_{\mathrm{avg}} \approx p_3 2\pi^2 f^2 B^2 = k_{\mathrm{eddy}} f^2 B^2,$$
$$(P_{\mathrm{hyst}})_{\mathrm{avg}} = (p_4|\dot{\mathbf{B}}|)_{\mathrm{avg}} \approx p_4 \frac{\pi}{2} f B = k_{\mathrm{hyst}} f B^2$$

with values $k_{\mathrm{eddy}} = 0.342\,\mathrm{W/m^3}$ and $k_{\mathrm{hyst}} = 196.83\,\mathrm{W/m^3}$. The value of $B = 1\,\mathrm{T}$ was selected as expected average flux density in the iron.

Supply Current

We analyze the effect of two different current pulse shapes shown in Fig. 2. These pulses can be generated via a switched resonance capacitor circuit [10] and feature an almost identical ramp between 2 ms and 3 ms. A total current of 47.5 kA is required to achieve the desired flux density of 1.8 T in the air gap. The parts of the cycle before and after the ramp are irrelevant for the acceleration of muons as they

ISBN: 978-3-95450-247-9 ISSN: 2673-5490 doi: 10.18429/JACoW-IPAC2024-TUPR54

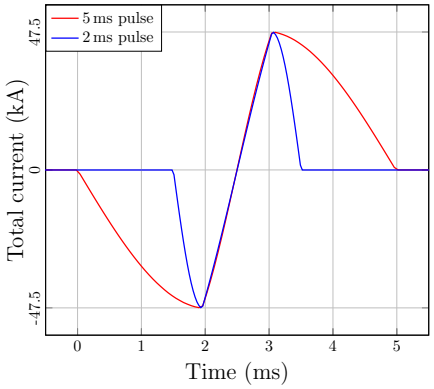

Figure 2: Input current pulse.

are injected and extracted at the peak flux densities. Two options are compared, where one prolongs the cycle to 5 ms (red), the other to 2 ms (blue). The magnetic flux density follows the cycle very closely.

Software

The numerical problem representation was generated and solved by the Python based finite element software Pyrit [11].

Results

The total loss is the sum of iron and copper loss and is shown in Fig. 3. In this analysis the 2 ms pulse causes a lower total loss. The corresponding copper loss is decreased by a factor of two. Removing heat of the iron core becomes more important for the 2 ms pulse since the dissipated energy in the iron core is higher by 28 J/m.

Figure 4 compares the *BH* loci of the anhysteretic model $H_y = \nu(B_y)B_y$ (dashed) to those obtained in the green point in the iron pole marked in Fig. 5. The shown *BH* paths start at zero and are followed counter clockwise. The ascending half of the plot shows the behaviour defined by the 1 ms ramp. The decreasing parts of the loop correspond to the preloading and relaxing phases of the cylce. They differ for both pulses such that the enclosed area and thereby the iron loss is higher in the case of a 2 ms pulse excitation. In addition, we note that the iron does not return to its initial

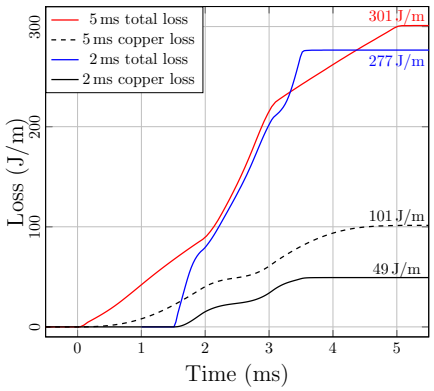

Figure 3: Lost energy during one cycle.

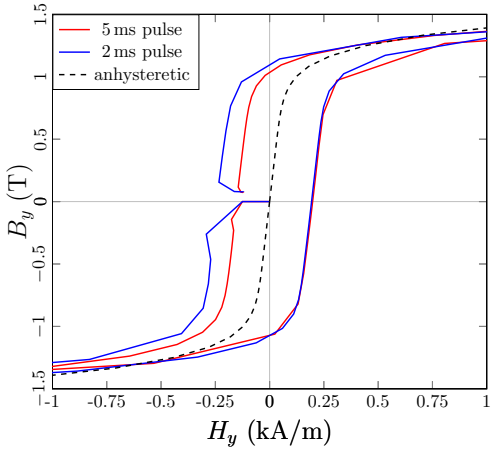

Figure 4: Hysteresis loop in a central point of the pole (green in Fig. 5).

unexcited state but rather remains magnetized in the second quadrant. The remaining magnetization will slightly offset the next ramping cycle.

For completeness, a plot of the magnetic flux density providing 1.8 T in the center of the air gap is shown in Fig. 5. The conductor contour is highlighted in white.

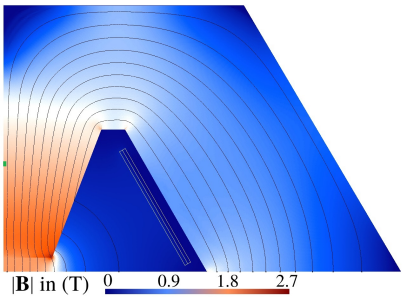

Figure 5: Magnetic flux density with 1.8 T in the center of the air gap. The conductor shape and a reference point in the pole are highlighted.

CONCLUSION

The procedure of simulating normal-conducting fast-ramping magnets has been layed out in this paper. Calculations for a preliminary muon collider dipole magnet have been conducted including eddy-current and hysteresis losses. It has been shown that, a trade-off between iron and copper loss can be achieved by changing the pulse duration.

ACKNOWLEDGEMENT

This work is funded by the Europen Union (EU) within the Horizon Europe Framework Programme (Project MuCol, grant agreement 101094300). Views and opinions expressed are however those of the author(s) only and do not necessarily reflect those of the EU or European Research Executive Agency (REA). Neither the EU nor the REA can be held responsible for them.

ISBN: 978-3-95450-247-9 ISSN: 2673-5490 doi: 10.18429/JACoW-IPAC2024-TUPR54

REFERENCES

[1] C. Accettura *et al.*, "Towards a muon collider", *The European Physical Journal C*, vol. 83, no. 9, Sep. 2023. doi:10.1140/epjc/s10052-023-11889-x

[2] IMCC, "A Design Study for a Muon Collider complex at 10 TeV centre of mass", 2023. https://muoncollider.web.cern.ch

[3] S. Fabbri *et al.*, "Magnets for a muon collider", in *Proc. IPAC'23*, Venice, Italy, May 2023, pp. 3712–3715. doi:10.18429/JACoW-IPAC2023-WEPM062

[4] J. S. Berg and H. Witte, "Pulsed synchrotrons for very rapid acceleration", in *AIP Conference Proceedings*, 2016. doi:10.1063/1.4965683.

[5] S. Schöps, H. De Gersem, and T. Weiland,"Winding functions in transient magnetoquasistatic field-circuit coupled simulations", *COMPEL*, vol. 32, no. 6, pp. 2063–2083, Nov. 2013. doi:10.1108/compel-01-2013-0004

[6] P. Dular *et al.*, "A 3-D magnetic vector potential formulation taking eddy currents in lamination stacks into account", *IEEE Transactions on Magnetics*, vol. 39, no. 3, pp. 1424–1427, May 2003. doi:10.1109/tmag.2003.810386

[7] V. C. Silva, G. Meunier, and A. Foggia, "A 3-D finite-element computation of eddy currents and losses in laminated iron cores allowing for electric and magnetic anisotropy", *IEEE Transactions on Magnetics*, vol. 31, no. 3, pp. 2139–2141, May 1995. doi:10.1109/20.376469

[8] F. Henrotte *et al.*, "Pragmatic two-step homogenisation technique for ferromagnetic laminated cores", *IET Science, Measurement Technology*, vol. 9, no. 2, pp. 152–159, Mar. 2015. doi:10.1049/iet-smt.2014.0201

[9] G. Bertotti, "General properties of power losses in soft ferromagnetic materials", *IEEE Trans. Magn.*, vol. 24, no. 1, pp. 621–630, Jan. 1988. doi:10.1109/20.43994

[10] D. Aguglia *et al.*, "A two harmonics circuit for the powering of the very fast RCS (Rapid Cycling Synchrotron) of the muon collider accelerator", in *Proc. IPAC'23*, Venice, Italy, May 2023, pp. 3746–3749. doi:10.18429/JACoW-IPAC2023-WEPM078

[11] J. Bundschuh, M. G. Ruppert, and Y. Späck-Leigsnering, "Pyrit: A finite element based field simulation software written in Python", *COMPEL*, vol. 42, no. 5, pp. 1007–1020, Sep. 2023. doi:10.1108/compel-01-2023-0013